We assume the I_{ij} to be uniform over a given segment, and perform the orbit average by averaging the products $c_ic_jI_{ij}$, with c_ic_j averaged over the given segment. The geometry involved is quite complex and only very rough numerical estimates of the integrals I_{ij} have been made, from which we conclude that

$$0.10<(\lambda^{(3)}-\lambda^{(2)})/\lambda^{(2)}<0.20.$$

The processes that contribute to these I_{ij} can be classified as, say, N (only longitudinal phonons involved) and U (both longitudinal and transverse phonons involved). Roughly $\frac{2}{3}$ of the above factor results from N processes, partly because there is some cancellation between contributions from U processes.

APPENDIX D

To calculate the pressure dependence of de Haas–van Alphen areas, we use the formula

$$\frac{d\ln A}{dP}=\frac{\partial\ln A}{\partial\ln n}\frac{d\ln n}{dP}+\frac{\partial\ln A}{\partial\ln\alpha}\frac{d\ln\alpha}{dP}+\sum_{G=1}^{3}\left(\frac{\partial\ln A}{\partial V_G}+\frac{\partial\ln A}{\partial\ln E_F}\frac{\partial\ln E_F}{\partial V_G}\bigg|_{\text{Vol}}\right)\frac{dV_G}{dP}.$$

The first two terms account for the changes in electron density n and ratio of lattice constants α. The last term accounts for the change in band gaps; $\partial\ln E_F/\partial\ln V_G|_{\text{Vol}}$ is the shift in Fermi energy, which accompanies a change in V_G in such a way that the Fermi surface encloses constant volume. The V_G's change according to (2), and we shall take into account possible changes in the parameter R_c with energy.

For the principal section of the β arm, we find that $d\ln A/dP=[4.41+5.10\eta]K_T$, where K_T is the compressibility and $\eta=d\ln R_c/d\ln E$. The various contributions are (in units of K_T): 0.67 from the electron density, 1.21 from the lattice constants,[18] and $2.25+3.94\eta$ from the band gaps. Comparing this with the result of Anderson, O'Sullivan, and Schirber, $d\ln A/dP=(3.4\pm0.15)K_T$, we would deduce that $\eta=-0.18$. We note however that uncertainty in this value for η is greater by a factor of four than experimental uncertainty in $d\ln A/dP$. Finally, we point out again that our calculations of $d\ln A/dP$ for second-zone orbits give numbers about 20% smaller than the experimental ones, as do the calculations of Anderson, O'Sullivan, and Schirber.

PHYSICAL REVIEW VOLUME 175, NUMBER 3 15 NOVEMBER 1968

Third-Order Elastic Constants of Aluminum*†

J. F. THOMAS, JR.‡
Department of Physics and Materials Research Laboratory, University of Illinois, Urbana, Illinois 61801
(Received 5 April 1968)

The complete set of six third-order elastic constants of single-crystal Al has been experimentally determined by measuring both hydrostatic-pressure and uniaxial-stress derivatives of the natural sound velocities using a two-specimen interferometric technique. The specimens were neutron-irradiated to eliminate dislocation effects from the uniaxial experiments. A self-consistent set of hydrostatic-pressure derivatives of the second-order elastic constants has been calculated from the measured third-order constants. The third-order elastic constants have also been used to calculate the thermal expansion in the anisotropic-continuum model at both high and low temperatures, and a comparison has been made with the directly measured expansion coefficients.

INTRODUCTION

HIGHER-ORDER elastic constants provide an efficient measure of many aspects of lattice anharmonicity. In particular, the third-order elastic constants are useful in the calculation of many mechanical and thermal properties related to the anharmonic nature of the lattice potential energy. In addition, the third-order elastic constants would be expected to provide useful new information on the nature of cohesive properties and interatomic forces.

The most powerful method for obtaining third-order elastic constants is the measurement of sound-velocity changes with applied homogeneous stress. Basic measurements of this type utilize simple modifications of the well-known megacycle pulse-echo technique. Early measurements were restricted to velocity change with applied hydrostatic pressure. For a cubic crystal, this gives three experimental numbers which are related to five of the six third-order elastic constants. To obtain sufficient information to measure all six third-order elastic constants, it is necessary to utilize a deviatoric stress such as uniaxial compression.

* This research was supported by the U. S. Atomic Energy Commission under Contract No. AT(11-1)-1198.
† Based on a thesis submitted in partial fulfillment of the requirements for the degree of Doctor of Philosophy at the University of Illinois, 1968.
‡ Present address: Department of Physics, University of Virginia, Charlottesville, Va. 22903.

Here, in the study of metal single crystals, a basic problem arises. Uniaxial compressions large enough to produce directly measurable changes in the transit time of an ultrasonic pulse will also likely produce changes in the dislocation network always present in the metal crystals. It is well known that dislocations will affect the measured sound velocity. If the applied uniaxial compression changes the existent dislocation network, for example by causing breakaway from weak pinning points or activation of dislocation sources, a dislocation contribution will be present in the measured sound-velocity stress derivative. Hence, one is restricted to very small uniaxial compressions, and a system of electronics capable of detecting relative sound-velocity changes of several parts per million (ppm) is required.

The first complete set of third-order elastic constants of a metal single crystal was obtained by Hiki and Granato.[1] They used the two-specimen interferometric technique[2] to measure the third-order elastic constants of the noble metals Cu, Ag, and Au. Their measurements included both hydrostatic- and uniaxial-stress derivatives. Swartz[3] used the same technique for measurements on β brass. Salama and Alers[4] repeated uniaxial-stress measurements on Cu at several temperatures using the sing-around method.[5] Their room-temperature values agree well with Hiki and Granato. They also completed measurements at helium temperatures, the only such measurements which exist at the present time for any material.

The third-order elastic constants of the noble metals[1,4] and β brass[3] confirm the expectation regarding useful information on interatomic forces. The results for these crystals correspond closely to those expected, if short-range, central forces make a predominant contribution to the higher-order elastic constants.[1,3] An important conclusion, then, is that the conduction electrons seem to play a minor role in the anharmonicity of these materials. This might be considered somewhat surprising, but can be understood in terms of the existence of overlapping electronic d shells and the resulting strong exchange forces.

It was decided to investigate a material in which the conduction electrons would be expected to make a major contribution to the higher-order elastic constants and, hence, to the anharmonic properties of the material. One such material is aluminum. In Al, there are no d electrons; the ion cores are small; and the exchange interactions between ion cores should be negligible. Also, Al has three valence electrons per atom. Hence, the Fermi surface will interact strongly with the Brillouin zone. The conduction electrons should contribute to the shear as well as the compressive elastic constants.

[1] Yosio Hiki and A. V. Granato, Phys. Rev. **144**, 411 (1966).
[2] R. P. Espinola and P. C. Waterman, J. Appl. Phys. **29**, 718 (1958).
[3] Karl D. Swartz, thesis, University of Illinois, 1966 (unpublished).
[4] K. Salama and G. A. Alers, Phys. Rev. **161**, 673 (1967).
[5] R. L. Forgacs, IEEE Trans. Instr. Methods **9**, 359 (1960).

SPECIMEN PREPARATION

The four aluminum single crystals used in this investigation were of dimensions 15×16×17 mm. They were oriented with faces perpendicular to [110], [1$\bar{1}$0], and [001] directions. These orientations were checked with Laüe back-reflection photographs and were found to be accurate to better than 1°. The crystals were obtained as oriented from Semi-Elements Inc., Saxonburg, Pa. Order-of-magnitude estimations of impurity concentrations were determined by emission spectroscopy, indicating that Cu, Fe, In, Ga, Ca, and Ti were present in concentrations of 10–100 ppm. Hence, we estimated that the crystals were between 99.95 and 99.99% pure Al. In order to make sound-velocity measurements by the use of a pulse-echo technique, it was necessary to polish the crystals so that opposite faces would be flat and parallel to better than 50 ppm. A convenient method has been developed to obtain such tolerances with moderate effort.[6]

The second-order elastic constants of the Al crystals were then measured using a direct pulse-echo technique. The results are presented in Table I and compared with the values of Schmunk and Smith[7] and Kamm and Alers.[8] For the particular orientation of our crystals, we were able to obtain eight measurements of four pure-mode velocities. The errors presented with our results in Table I represent the consistency of these eight measurements as derived from a least-squares fit of the data. The small consistency error is taken as a final indication that the Al specimens were well-oriented single crystals with no important lineage structure.

During the course of the investigation, it was decided to neutron-irradiate two of the Al crystals. The irradiation took place in the CP-5 reactor at the Argonne National Laboratory. The integrated exposure was approximately 5×10^{18} neutrons per cm^2 with energy greater than 100 keV. The temperature of the crystals was neither monitored nor controlled during the irradiation.

EXPERIMENTAL PROCEDURE

For measurement of the sound-velocity stress derivatives, we have used the two-specimen ultrasonic interferometric technique. The method and apparatus are basically the same as those described by Hiki and Granato[1] and by Swartz.[3] A further analysis of some aspects of the measurement found to be particularly important in this experiment has been given by the author elsewhere.[9]

The measurements have been analyzed within the formulation developed by Thurston and Brugger.[10]

[6] T. L. Ochs (to be published).
[7] R. E. Schmunk and Charles S. Smith, J. Phys. Chem. Solids **9**, 100 (1959).
[8] G. N. Kamm and G. A. Alers, J. Appl. Phys. **35**, 327 (1964).
[9] J. F. Thomas, Jr., thesis, University of Illinois, 1968 (unpublished).
[10] R. N. Thurston and K. Brugger, Phys. Rev. **133**, A1604 (1964).

TABLE I. The second-order elastic constants of Al at 25°C. The errors indicated in column 2 represent the consistency of the measured values. (Units of 10^{12} dyn cm^{-2}.)

c	This experiment	Schmunk and Smith[a]	Kamm and Alers[b]
C_{11}	1.0675±0.0005	1.0732	1.0686
C_{12}	0.6041±0.0008	0.6094	0.6075
C_{44}	0.2834±0.0004	0.2832	0.2824

[a] Reference 7.
[b] Reference 8.

They defined a quantity called the natural velocity, $W=2L_0/t$, where L_0 is the path length in the unstressed crystal and t is the round-trip transit time. They then evaluated the derivative $(\partial/\partial P)(\rho_0 W^2)_{T,P=0}$ in terms of linear combinations of the second- and third-order elastic constants for various combinations of pure sound modes and applied stress P. Here ρ_0 is the density of the unstressed medium. But $(\rho_0 W^2)$ will vary with stress simply as t^{-2}. The formulation is convenient because we no longer need to worry about the path length in the stressed crystal.

The stress derivative discussed above can be written as

$$\frac{\partial}{\partial P}(\rho_0 W^2)_{T,P=0}=2w\left(\frac{1}{W}\frac{\partial W}{\partial P}\right)_{T,P=0}. \tag{1}$$

Here w is the second-order elastic constant $(\rho_0 W^2)$ evaluated at zero stress and is given by an appropriate linear combination of the constants given in Table I. If we consider W to be a simple thermodynamic function of two variables, $W=W(P,T)$, then

$$\frac{1}{W}\frac{\partial W}{\partial P}\bigg|_T=-\frac{1}{W}\frac{\partial W}{\partial T}\bigg|_P\frac{\partial T}{\partial P}\bigg|_W. \tag{2}$$

Equation (2) indicates the procedure we followed in measuring natural-velocity stress derivatives using the two-specimen interferometric technique. We first measured $(1/W)(\partial W/\partial T)|_P$ for a particular sound mode. This could be considered as a calibration of the interferometer for this mode. We then measured $(\partial T/\partial P)|_W$ for the various stress derivatives of the mode. A detailed account of these measurements is contained in Ref. 9.

The results for the natural-velocity temperature derivatives can be expressed in terms of the temperature dependence of the usual second-order elastic constants, $c=\rho v^2$. Here ρ is the density, and v is the actual sound velocity. Hence, the temperature dependence of c is given by

$$\frac{\partial c}{\partial T}\bigg|_P=c\left(\frac{2}{W}\frac{\partial W}{\partial T}\bigg|_P-\alpha\right). \tag{3}$$

Here α is the coefficient of linear thermal expansion (0.234×10^{-4} °C^{-1} for Al at 25°C).[11] The results for

[11] C. S. Taylor, L. A. Willey, Dana W. Smith, and Junius D. Edwards, Metals & Alloys **9**, 189 (1938).

TABLE II. The temperature derivatives of the second-order elastic constants of Al at 25°C. (Units of 10^8 dyn cm^{-2} °C^{-1}.)

	$(\partial c/\partial T)_P$		
c	This experiment	Long and Smith[a]	Kamm and Alers[b]
C_{11}	−3.51	−3.44	−3.75
C_{12}	−0.67	−0.98	−0.55
C_{44}	−1.45	−1.43	−1.43

[a] Reference 12.
[b] Reference 8.

$(\partial c/\partial T)|_P$ are presented in Table II and are compared to the results of Long and Smith[12] and Kamm and Alers.[8] Kamm and Alers present their results in tabular form, and we have calculated the derivative from their high-temperature values.

The sensitivity of the two-specimen technique depends upon the smallest wave-velocity change which will produce an observable change in an ultrasonic interference pattern. This, in turn, depends upon the structure of the pattern and the position in time at which measurements are being obtained. In general, the sensitivity is higher at longer transit times. We have observed that changes of the order $\delta W/W=2\times10^{-6}$ can be detected for waves which have spent 100–150 μsec in the crystals. Extensive measurements by Swartz[13] on NaCl have demonstrated that the two-specimen interferometer gives reliable results compatible with one-specimen techniques. The two-specimen technique has the distinct advantage that small temperature drifts of the stressed specimen will not obscure or effect the sound-velocity change with pressure.

EVALUATION OF THIRD-ORDER ELASTIC CONSTANTS

For the particular orientation of our crystals, we were able to investigate five different pure-mode sound waves, two longitudinal and three transverse. We measured the hydrostatic-pressure derivatives of the natural velocities of these five waves. We also measured nine uniaxial-stress derivatives of the five natural velocities. These 14 experiments are characterized in Table III.

Thurston and Brugger[10] have given explicit relations between the measured quantities $(\partial/\partial P)(\rho_0 W^2)_{T,P=0}$ and the second- and third-order elastic constants for the 14 experiments described in Table III. These relations are presented in Table IV. In Table IV, the superscript T indicates an isothermal elastic constant. The third-order elastic constants are all of the mixed type, being derived from an isothermal strain derivative of an adiabatic second-order elastic constant.

We first measured the hydrostatic-pressure derivatives of the five natural sound velocities, experiments 10–14 of Tables III and IV. Measurements were taken

[12] T. R. Long and C. S. Smith, J. Acoust. Soc. Am. **26**, 146 (1954).
[13] Karl D. Swartz, J. Acoust. Soc. Am. **41**, 1083 (1967).

TABLE III. Characterization of sound-velocity stress experiments.

Expt. No.	Propagation direction N	Displacement direction U	Stress direction M	$w=(\rho_0 W^2)_{P=0}$
1	[110]	[110]	[001]	$\frac{1}{2}C_{11}+\frac{1}{2}C_{12}+C_{44}$
2	[110]	[1$\bar{1}$0]	[001]	$\frac{1}{2}C_{11}-\frac{1}{2}C_{12}$
3	[110]	[001]	[001]	C_{44}
4	[001]	[001]	[110]	C_{11}
5	[001]	[110]	[110]	C_{44}
6	[001]	[1$\bar{1}$0]	[110]	C_{44}
7	[110]	[110]	[1$\bar{1}$0]	$\frac{1}{2}C_{11}+\frac{1}{2}C_{12}+C_{44}$
8	[110]	[1$\bar{1}$0]	[1$\bar{1}$0]	$\frac{1}{2}C_{11}-\frac{1}{2}C_{12}$
9	[110]	[001]	[1$\bar{1}$0]	C_{44}
10	[001]	[001]	Hyd.	C_{11}
11	[001]	any $\perp$N	Hyd.	C_{44}
12	[110]	[110]	Hyd.	$\frac{1}{2}C_{11}+\frac{1}{2}C_{12}+C_{44}$
13	[110]	[1$\bar{1}$0]	Hyd.	$\frac{1}{2}C_{11}-\frac{1}{2}C_{12}$
14	[110]	[001]	Hyd.	C_{44}

on two sets of crystals, and the results for each mode were averaged. The natural sound-velocity change for a typical hydrostatic experiment is illustrated in Fig. 1. The results were expressed in terms of three linear combinations of five of the six third-order elastic constants, $(C_{111}+2C_{112})$, $(\frac{1}{2}C_{111}-\frac{1}{2}C_{123})$, and $(C_{144}+2C_{166})$. These three numbers were determined by a least-squares fit of the five measurements. The results are presented in the first row of Table V. The error indicated with these results represents the consistency of the five measurements.

TABLE IV. Natural sound-velocity stress derivatives as a function of second- and third-order elastic constants.

Expt. No.	$(\partial/\partial P)(\rho_0 W^2)_{T,P=0}$
1	$2wa+\frac{1}{2}aC_{111}+\frac{1}{2}(3a-b)C_{112}-\frac{1}{2}bC_{123}$ $-bC_{144}+2aC_{166}$
2	$2wa+\frac{1}{2}aC_{111}-\frac{1}{2}(a+b)C_{112}+\frac{1}{2}bC_{123}$
3	$-2wb+aC_{144}+(a-b)C_{166}$
4	$2wa+aC_{111}+(a-b)C_{112}$
5	$w(a-b-2c)+\frac{1}{2}(a-b)C_{144}+\frac{1}{2}(3a-b)C_{166}-2cC_{456}$
6	$w(a-b+2c)+\frac{1}{2}(a-b)C_{144}+\frac{1}{2}(3a-b)C_{166}+2cC_{456}$
7	$w(a-b+2c)+\frac{1}{4}(a-b)C_{111}+\frac{1}{4}(5a-3b)C_{112}+\frac{1}{2}aC_{123}$ $+aC_{144}+(a-b+4c)C_{166}$
8	$w(a-b-2c)+\frac{1}{4}(a-b)C_{111}+\frac{1}{4}(a+b)C_{112}-\frac{1}{2}aC_{123}$
9	$2wa+\frac{1}{2}(a-b)C_{144}+\frac{1}{2}(3a-b)C_{166}+2cC_{456}$
10	$-1+2w(2a-b)+(2a-b)[C_{111}+2C_{112}]$
11	$-1+2w(2a-b)+(2a-b)[C_{144}+2C_{166}]$
12	$-1+2w(2a-b)+(2a-b)[\frac{1}{2}C_{111}+2C_{112}$ $+\frac{1}{2}C_{123}+C_{144}+2C_{166}]$
13	$-1+2w(2a-b)+(2a-b)[\frac{1}{2}C_{111}-\frac{1}{2}C_{123}]$
14	$-1+2w(2a-b)+(2a-b)[C_{144}+2C_{166}]$

$a=\dfrac{C_{12}^T}{3B^T(C_{11}^T-C_{12}^T)}$, $b=\dfrac{C_{11}^T+C_{12}^T}{3B^T(C_{11}^T-C_{12}^T)}$, $c=\dfrac{1}{4C_{44}}$,

$3B^T=C_{11}^T+2C_{12}^T$,

$C_{11}^T=1.0339\times10^{12}$ dyn cm^{-2},

$C_{12}^T=0.5104\times10^{12}$ dyn cm^{-2}

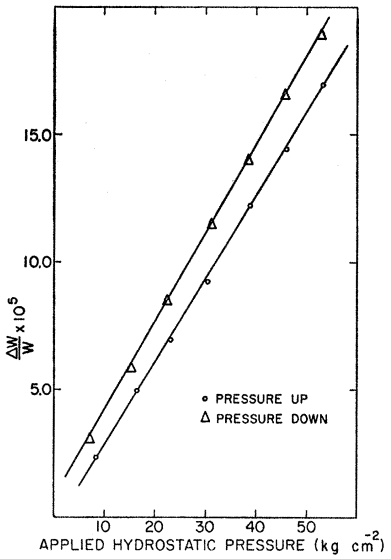

FIG. 1. Natural velocity change versus hydrostatic pressure for a C_{44} mode (experiment 14 of Tables III and IV). The separation between the curves for increasing and decreasing pressure is due to a thermal lag between the surface and bulk of the specimen of approximately 0.1°C. To reduce any effect on the measured slope, the results for increasing and decreasing pressure were averaged.

Initial uniaxial-stress measurements were made on the two sets of crystals. The stress range was approximately 0–40 kg cm^{-2}. Even in this small stress region, we expected that dislocation motion might occur. Hiki and Granato[1] found that an initial prestress was effective in eliminating dislocation effects in measurements on noble metals. That method was also attempted here. The sound-wave attenuation was monitored during the prestress, and no significant changes were detected. However, it became apparent that dislocation effects were present in the initial uniaxial data.

The problem of determining whether or not dislocation effects exist in a particular uniaxial experiment or series of experiments is quite involved. Initially, it was hoped that for any particular experiment a dislocation contribution would be a nonlinear function of applied stress, easily distinguishable from the patently linear lattice effect. Hiki and Granato[1] observed a highly nonlinear velocity change at stresses above their prestress level. However, Salama and Alers[4] discounted this simple notion. Their measurements on hardened Cu crystals showed that the uniaxial data could be linear, reproducible, show no hysteresis, and give no attenu-

TABLE V. The third-order elastic constants related to sound-velocity hydrostatic-pressure derivatives. The errors indicated represent the consistency of each set of measurements. (Units of 10^{12} dyn cm^{-2}.)

Measurement	$C_{111}+2C_{112}$	$\frac{1}{2}C_{111}-\frac{1}{2}C_{123}$	$C_{144}+2C_{166}$
Hydrostatic	-17.10 ± 0.05	-5.60 ± 0.07	-6.99 ± 0.04
Uniaxial	-17.11 ± 0.04	-5.57 ± 0.02	-7.06 ± 0.01

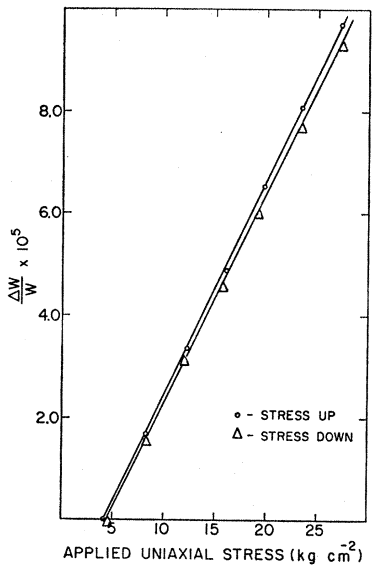

FIG. 2. Natural velocity change versus applied uniaxial stress for a C_{44} mode (experiment 3 of Tables III and IV). The experiment was begun with a 4-kg-cm^{-2} setting stress applied to the specimen.

ation change with applied stress and could still contain a dislocation contribution. However, they suggested that a suitable criterion for the absence of dislocation effects in a series of uniaxial measurements was that hydrostatic-pressure derivatives calculated from the uniaxial data be in agreement with the directly measured values.

We have adopted that criterion here. This is reflected in the method of data reduction. The nine uniaxial-stress experiments give information on eight linear combinations of the six third-order elastic constants. The uniaxial data could be used alone to obtain a set of third-order elastic constants. The three linear combinations related to the hydrostatic pressure derivatives could then be calculated from this set. If substantial agreement could be obtained between the measured and calculated values of these three linear combinations, then it would be proper to combine all the data and obtain a self-consistent set of third-order elastic constants and hydrostatic pressure derivatives.

The dominant characteristic of the initial uniaxial data was that experiments 1, 2, 3, 4, 7, and 8 gave a linear dependence of the change in natural velocity with stress while experiments 5, 6, and 9 did not. A typical linear natural-velocity change is illustrated in Fig. 2. In the nonlinear experiments, a hysteresis effect was observed which was qualitatively reproducible. A typical nonlinear natural-velocity change including hysteresis is illustrated in Fig. 3.

The six linear experiments were related to five of the six third-order elastic constants. These were the same five constants which determined the hydrostatic-pressure derivatives. The initial uniaxial data from the six linear experiments was used to determine these five elastic constants by a least-squares analysis. The set of third-order constants so determined was totally inconsistent with the measured hydrostatic-pressure derivatives. For example, after a particular set of measurements, we obtained $(C_{111}+2C_{112})=-8.20\times10^{12}$ dyn cm^{-2} compared to the measured value of -17.10 in the same units. Dislocation effects were obviously present in the nonlinear experiments. It was concluded that dislocation effects must also have been present in several of the linear experiments.

One set of Al crystals was then neutron-irradiated as described previously. The uniaxial-stress measurements were then repeated. Results for experiments 2, 3, 5, 6, and 9 were essentially unchanged. The hysteresis effects observed in the latter three of these experiments were still present. The results for experiments 1, 4, 7, and 8 changed substantially. The measured natural-velocity changes with stress all became algebraically larger. This is the direction of change one would expect if dislocation effects had been eliminated. The six linear experiments were again analyzed to obtain a least-squares fit for five of the six third-order elastic constants. The three linear combinations of the third-order elastic constants related to the hydrostatic pressure derivatives calculated from these results agreed almost exactly with the measured values. These combinations are presented in the second row of Table V. The error presented represents the consistency of the six uniaxial measurements.

Results of experiments 5, 6, and 9 on the irradiated crystals still showed hysteresis effects similar to that illustrated in Fig. 3. It is very likely that the observed hysteresis effects are associated with microscopic plastic flow. Some dislocation motion must still be

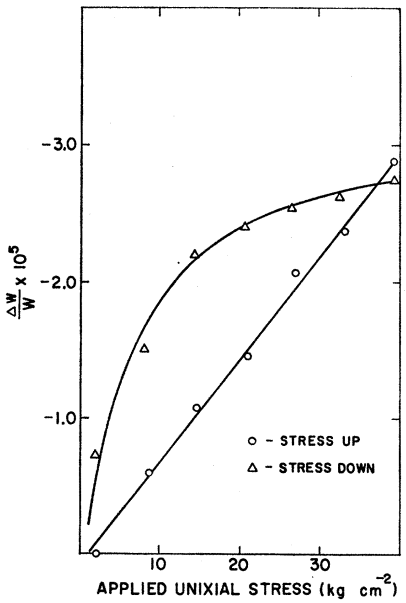

FIG. 3. Natural velocity change versus applied uniaxial stress for a typical nonlinear mode (experiment 9 of Tables III and IV). The observed hysteresis is attributed to a dislocation effect.

TABLE VI. Experimental data and results for natural-velocity stress derivatives. The errors indicated in column 4 represent the range of the measured values.

Expt. No.	w (dyn cm^{-2})	$\frac{1}{W}\frac{\partial W}{\partial T}\Big\|_P$ (°C^{-1})	$\frac{\partial T}{\partial P}\Big\|_W$ (°C dyn^{-1} cm^2)	$\frac{1}{W}\frac{\partial W}{\partial P}\Big\|_T$ (dyn^{-1} cm^2)	$\frac{\partial}{\partial P}(\rho_0 W^2)_{T,P=0}$ (dimensionless)
1	1.1192×10^{12}	-1.47×10^{-4}	$-1.74\pm0.10\times10^{-8}$	$-2.56\pm0.14\times10^{-12}$	-5.73 ± 0.32
2	0.2317	−2.95	0.66±0.04	1.95±0.13	0.90±0.06
3	0.2834	−2.44	1.78±0.07	4.34±0.16	2.46±0.09
4	1.0675	−1.53	−0.51±0.05	−0.78±0.08	−1.67±0.16
7	1.1192	−1.47	−1.04±0.07	−1.53±0.10	−3.42±0.22
8	0.2317	−2.95	0.23±0.02	0.68±0.04	0.32±0.02
10	1.0675	−1.53	1.80±0.10	2.75±0.15	5.87±0.32
11, 14	0.2834	−2.44	1.40±0.02	3.42±0.05	1.94±0.03
12	1.1192	−1.47	1.98±0.02	2.91±0.02	6.51±0.05
13	0.2317	−2.95	1.01±0.05	2.98±0.15	1.38±0.07

occurring in the irradiated crystals. However, because of the excellent agreement observed in Table V between uniaxial and hydrostatic measurements, we conclude that dislocation effects have been effectively eliminated from the six linear uniaxial experiments.

We then combined the acceptable uniaxial and hydrostatic data to obtain a self-consistent set of third-order elastic constants and hydrostatic-pressure derivatives. The data used in this calculation are summarized in columns 2–4 of Table VI. Results for the natural-velocity stress derivatives [Eq. (2)] are presented in the fifth column, and for $(\partial/\partial P)(\rho_0 W^2)_{T,P=0}$ [Eq. (1)] in the sixth column of this table. The errors presented with the measured $(\partial T/\partial P)|_W$ represent the range of several measurements for each mode (on the irradiated crystals only for uniaxial measurements). These numbers are simply scaled to obtain the error presented in the fifth and sixth columns. From the relations of Thurston and Brugger[10] (Table IV) and the measured quantities $(\partial/\partial P)(\rho_0 W^2)_{T,P=0}$, we obtained the five third-order elastic constants related to the hydrostatic and linear uniaxial data by a least-squares analysis. The final set of third-order elastic constants is presented in Table VII. The errors indicated in Table VII represent the range of measured stress derivatives. These were obtained by substituting various combinations of the maximum and minimum pressure derivatives in the least-squares computer program and noting the range of third-order elastic constants so calculated.

Although experiments 5, 6, and 9 were grossly nonlinear, certain restrictions on the stress derivative could be deduced. It was clear that the derivative was small in each case. Assuming that the constants C_{144} and C_{166} were well known, a fair estimate of the remaining third-order elastic constant C_{456} could be obtained. This value of C_{456} is presented in Table VII.

TABLE VII. The third-order elastic constants of Al at 25°C. The errors represent the range of measured stress derivatives as discussed in the text. (Units of 10^{12} dyn cm^{-2}.)

$C_{111}=$	-10.76 ± 0.30
$C_{112}=$	-3.15 ± 0.10
$C_{123}=$	$+0.36\pm0.15$
$C_{144}=$	-0.23 ± 0.05
$C_{166}=$	-3.40 ± 0.10
$C_{456}=$	-0.30 ± 0.30

The final self-consistent set of third-order elastic constants was used to calculate the hydrostatic-pressure derivatives of the adiabatic second-order elastic constants, $c=\rho v^2$. From the definitions of c and W, we determine that

$$\frac{\partial c}{\partial P}\Big|_{T,P=0}=\frac{c}{3B^T}+\frac{\partial}{\partial P}(\rho_0 W^2)_{T,P=0}. \tag{4}$$

Here B^T is the isothermal bulk modulus. The second term of Eq. (4) was calculated from the relations in Table IV (experiments 10–14) and the measured elastic constants. The results are presented in Table VIII and compared to the results of Schmunk and Smith.[7] The error presented is consistent with the error associated with the final set of third-order constants. Our values for the pressure derivatives of the shear constants (C_{44}, $\frac{1}{2}C_{11}-\frac{1}{2}C_{12}$) are in fair agreement with those of Schmunk and Smith. For the longitudinal constants (C_{11}, $\frac{1}{2}C_{11}+\frac{1}{2}C_{12}+C_{44}$), our results are significantly smaller. We have no definite explanation for this. In the following section, we investigate this comparison further by using the pressure-derivative results to calculate the lattice thermal expansion.

THERMAL EXPANSION AND THE GRÜNEISEN PARAMETER

Within the anisotropic continuum model, the thermal expansion can be calculated from the third-order elastic constants. For a cubic crystal, the thermal expansion is isotropic and can be expressed in terms of the pressure derivatives of the three second-order elastic constants. Hence, it depends directly upon the three linear combinations of the third-order elastic constants previously discussed (Table V). Comparison of a measured and calculated thermal expansion should provide some information on the magnitude of these three third-order constants.

TABLE VIII. The hydrostatic-pressure derivatives of the adiabatic second-order elastic constants, $c=\rho v^2$, of Al. The error presented with the results of the experiment is consistent with the error associated with the final set of third-order elastic constants.

c	$(\partial c/\partial P)\|_T$ This experiment	Schmunk and Smith[a]
C_{11}	6.35±0.23	7.35
C_{12}	3.45±0.16	4.11
C_{44}	2.10±0.12	2.31
$\frac{1}{2}C_{11}+\frac{1}{2}C_{12}+C_{44}$	7.00±0.31	8.04
$\frac{1}{2}C_{11}-\frac{1}{2}C_{12}$	1.45±0.10	1.62
$\frac{1}{3}C_{11}+\frac{2}{3}C_{12}$	4.42±0.18	5.19

[a] Reference 7.

We have calculated the thermal expansion within the quasiharmonic approximation. This means that all thermodynamic and elastic properties of a crystal are assumed to be determined by the harmonic lattice frequency distribution and its dependence on volume or, more generally, on strain. This dependence is usually specified by defining the scalar-mode Grüneisen parameters,

$$\gamma_i=-\frac{V}{\nu_i}\frac{d\nu_i}{dV}. \tag{5}$$

Here V is the volume of the material, and ν_i is the frequency of the ith normal mode. Within the quasiharmonic approximation, a thermodynamic Grüneisen parameter can be defined as a weighted mean of the individual mode parameters, namely,

$$\gamma=\sum_{i=1}^{3N} C_i\gamma_i \Big/ \sum_{i=1}^{3N} C_i. \tag{6}$$

Here C_i is the specific heat of the ith normal mode. γ is then directly related to the thermal expansion as[14]

$$\gamma=\beta V B_T/C_V=\beta V B_S/C_P. \tag{7}$$

Here β is the volume thermal expansion; V is the molar volume; B_T and B_S are, respectively, the isothermal and adiabatic bulk moduli; and C_V and C_P are, respectively, the specific heats at constant volume and constant pressure. We see that the calculation of the thermal expansion basically reduces to the calculation of the various γ_i and their weighted mean γ. It is convenient to compare measured and calculated values of the thermal expansion through the respective Grüneisen parameters.

In the quasiharmonic approximation, the mode parameters are not explicitly temperature-dependent. However, the thermodynamic parameter does depend on temperature through the weighting factors (specific heats C_i). Expressions for the high-temperature and low-temperature limits of the thermodynamic Grüneisen parameter can be obtained from Eq. (6). At high temperatures, $C_i=k$ (the Boltzmann constant) for each of the $3N$ modes, and

$$\gamma_H=\frac{1}{3N}\sum_{i=1}^{3N}\gamma_i. \tag{8}$$

At low temperatures, assuming the continuum model, it can be shown that[15]

$$\gamma_L=\sum_{i=1}^{3N}\frac{\gamma_i}{v_i^3}\Big/\sum_{i=1}^{3N}\frac{1}{v_i^3}. \tag{9}$$

Here v_i is the wave velocity of the ith mode.

The mode Grüneisen parameters of Al have been calculated within the anisotropic continuum model. γ_H and γ_L were then calculated from Eqs. (8) and (9). These calculations were performed according to a program described in detail elsewhere.[16] Results for γ_H and γ_L calculated from our elastic data (Table VII) are presented in the first column and from the elastic data of Schmunk and Smith[7] (Table VIII) in the second column of Table IX.

We also computed γ_H and γ_L from the measured thermal properties, according to Eq. (7). For γ_H, thermal values were taken at 25°C. The particular values used were as follows: the thermal expansion of Taylor *et al.*[11] ($\beta=0.702\times10^{-4}$ °C^{-1}), the bulk modulus measured here ($B_S=0.7585\times10^{12}$ dyn cm^{-2}), the molar volume from the x-ray lattice parameter data of Figgens *et al.*[17] ($V=10.004$ cm^3 per mole), and the specific heat of Giaque and Meads[18] ($C_P=24.34\times10^7$ erg °C^{-1} per mole). The γ_H computed from these values is presented in the third column of Table IX.

At low temperatures, contributions to the thermal expansion and the specific heat arise from both the lattice and the electron gas. Equation (7) can be separated in the form[19]

$$\gamma=(1/C_P)(C_l\gamma_l+C_e\gamma_e),$$

with

$$\gamma_l=\beta_l B_S V/C_l,\quad \gamma_e=\beta_e B_S V/C_e. \tag{10}$$

TABLE IX. The thermodynamic Grüneisen parameters of Al.

	From elastic data This experiment	From elastic data Schmunk and Smith[a]	From thermal data
γ_H	2.27	2.56	2.19
γ_L	2.33	2.60	2.45

[a] Reference 7.

[14] J. C. Slater, *Introduction to Chemical Physics* (McGraw-Hill Book Co., New York, 1939), p. 215.

[15] F. W. Sheard, Phil. Mag. **3**, 1381 (1958).

[16] Yosio Hiki, J. F. Thomas, Jr., and A. V. Granato, Phys. Rev. **153**, 764 (1967).

[17] B. F. Figgens, G. O. Jones, and D. P. Riley, Phil. Mag. **1**, 747 (1956).

[18] W. F. Giaque and P. F. Meads, J. Am. Chem. Soc. **63**, 1897 (1941).

[19] J. H. O. Varley, Proc. Roy. Soc. (London) **A283**, 413 (1956).

Here subscript l refers to the lattice, and subscript e to the electron gas. We must compute $\gamma_l=\gamma_L$ as it is this quantity which is calculated from the elastic data. At low temperatures, the thermal expansion and the specific heat depend on temperature as[20]

$$\beta(\text{or } C)=AT+BT^3. \quad (11)$$

The linear term in temperature is a measure of the electron-gas contribution. The cubic term in temperature is a measure of the lattice contribution, and this term must be isolated. The particular values used were as follows: the thermal expansion of White as reported by Collins and White[20] ($\beta/T^3=2.6\times10^{-11}$ °C^{-4}), the bulk modulus at 0°K of Kamm and Alers[7] ($B=0.7938\times10^{12}$ dyn cm^{-2}), the molar volume from the lattice parameter data of Figgens *et al.*[17] extrapolated to 0°K ($V=9.8724$ cm^3 per mole), and the specific heat of Phillips[21] [$(C/T^3)=2.468\times10^2$ erg °C^{-4} per mole]. The γ_L computed from these values is also presented in column 3 of Table IX.

There are two comparisons of interest in Table IX, the absolute magnitudes and the dispersion ($\gamma_H-\gamma_L$). The continuum model should give excellent agreement between the elastic and thermal values of γ_L. Unfortunately, the comparison for γ_L is difficult to assess due to large uncertainties (approximately 10%) in the measured thermal expansion. Agreement for γ_H should be questionable as the high frequency lattice modes must be considered. However, results for noble metals[16,22] show that good agreement is obtained between elastic and thermal values of γ_H. If this agreement could be expected for close packed metals in general, the values of γ_H in Table IX would favor our elastic data versus that of Schmunk and Smith.[7] With regard to the dispersion $\gamma_H-\gamma_L$, Barron[23] has shown that for a cubic, close-packed lattice with central forces between nearest neighbors only, $\gamma_H-\gamma_L=0.30$. Also, this difference becomes smaller when more distant neighbors must be taken into account. Measurements by Carr *et al.*[24] for Cu agree closely with this result. They obtain $\gamma_H-\gamma_L=0.28$ from thermal data. Elastic data will give $\gamma_H-\gamma_L=0.20$. This is consistent with the observation of Hiki and Granato[1] that the elastic properties of the noble metals are determined primarily by the exchange repulsion between ion cores. In Al, the elastic properties are determined primarily by the conduction electrons. Hence, one would expect that, in a force-constant picture, distant neighbors would be of importance. It is interesting to observe in Table IX that both the thermal and elastic Grüneisen parameters give $\gamma_H-\gamma_L<0$.

DISCUSSION AND CONCLUSIONS

We have determined the complete set of six third-order elastic constants of single crystal Al by measuring both hydrostatic-pressure and uniaxial-stress derivatives of the natural sound velocities. The specimens were neutron-irradiated to eliminate dislocation effects from the uniaxial experiments. A self-consistent set of hydrostatic-pressure derivatives of the second-order elastic constants calculated from the measured third-order elastic constants is in fair agreement with the measured values of Schmunk and Smith.[7] Values of the thermal expansion at both high and low temperatures calculated from our third-order elastic constants agree well with the directly measured expansion coefficients.

The observed pattern among the third-order elastic constants should allow some statement to be made regarding the cohesive properties of Al. The third-order elastic constants of the noble metals[1,4] recently obtained correspond closely to those expected, if short-range, central forces make a predominant contribution to the higher-order elastic constants.[1] Unfortunately, the situation for Al is not this simple. Leigh[25] has shown that the second-order elastic shear constants of Al can be accounted for by considering contributions from the electrostatic energy and the energy of the electron gas. In particular, C_{44} is related to the difference of large and nearly equal contributions from each of these energy terms. An extension of this calculation to the third order has indicated that similar considerations hold for the third-order constants and that, in addition, these constants depend on the complicated energy band structure of Al near the Brillouin zone edges and corners.[9] The contribution of the electrostatic energy to the third-order elastic constants is known.[9,26] We still require, however, a calculation of the energy of the electron gas which will include a satisfactory treatment of band-structure effects. Work now in progress[26] has indicated that a pseudopotential approach should be applicable to this problem.

ACKNOWLEDGMENTS

The author wishes to express his gratitude for the guidance and encouragement of his thesis adviser, Professor A. V. Granato. He would also like to thank Professor Y. Hiki for introducing him to the experimental techniques, and T. L. Ochs for his skillful assistance with the sample preparation.

[20] J. G. Collins and G. K. White, in *Progress in Low Temperature Physics*, edited by C. J. Gorter (North-Holland Publishing Co., Amsterdam, 1964).
[21] N. E. Phillips, Phys. Rev. **114**, 676 (1959).
[22] J. G. Collins, Phil. Mag. 8, 323 (1963).
[23] T. H. K. Barron, Phil. Mag. 46, 720 (1955).
[24] R. H. Carr, R. D. McGammon, and G. K. White, Proc. Roy. Soc. (London) **A280**, 72 (1964).
[25] R. S. Leigh, Phil. Mag. 42, 139 (1951).
[26] Tetsuro Suzuki (private communication).